entation to that of its corresponding K^+ ion in K_{12}-A,[3] and is consistent with its environment. The position of Rb(3) cannot be governed by electrostatics alone; Laplace's equation, $\nabla^2 V = 0$, implies that no purely electrostatic minimum for Rb(3) can exist in any intrazeolitic void. Apparently, the usual chemical attractive and repulsive forces have balanced to give a shallow energy minimum at an unusual position.

The three Rb(2) ions are located at the centers of the 8-oxygen rings, filling that equipoint, at sites of D_{4d} symmetry. The shortest Rb(2)–O distance is long by 0.4 Å,[5] indicating that these ions are "loosely bound". This was observed spectroscopically[8] in hydrated partially Rb^+-exchanged zeolite A, and crystallographically in both hydrated and dehydrated Cs_7Na_5-A.[1]

For zero-coordinate cations to occur, the zeolite must have a high Al/Si ratio, which leads to a high anionic charge density. This ratio is 1.0 in zeolite A, its maximum value according to Loewenstein's rule.[9] Secondly, large monovalent cations are required which "coat" the inner surface of the zeolite, filling all possible coordination sites before all negative charges of the framework have been balanced. In dehydrated K_{12}-A[3] and $Rb_{11}Na_1$-A, only 11 cations per unit cell can locate at sites in conventional contact with the zeolite framework. The twelfth negative charge is balanced by a cation for which no framework coordination site remains available, as in the children's game, "musical chairs".

These results allow us to employ a stringent definition of noncoordination. If the distance between two ions exceeds the sum of their corresponding radii by more than 1.0 Å, then these ions may be considered not bonded or uncoordinated. At least, their bond order is much less than one. On this basis, Rb(3) is termed zero-coordinate, zero being the sum of integers, all zero, describing its bond orders to its nearest neighbors. For this particular structure, the rounded-off value of 1.0 Å used in the criterion stated above may be raised to 1.5 Å.

References and Notes

(1) T. B. Vance, Jr., and K. Seff, *J. Phys. Chem.*, **79**, 2163 (1975).
(2) The nomenclature refers to the contents of the unit cell. For example, Cs_7Na_5-A represents $Cs_7Na_5Al_{12}Si_{12}O_{48}$, exclusive of water molecules if a hydrated crystal is considered.
(3) P. C. W. Leung, K. B. Kunz, I. E. Maxwell, and K. Seff, *J. Phys. Chem.*, **79**, 2157 (1975).
(4) A discussion of zeolite nomenclature is available: (a) R. Y. Yanagida, A. A. Amaro, and K. Seff, *J. Phys. Chem.*, **77**, 805 (1973); (b) L. Broussard and D. P. Shoemaker, *J. Am. Chem. Soc.*, **82**, 1041 (1960).
(5) "Handbook of Chemistry and Physics", 54th ed, The Chemical Rubber Company, Cleveland, Ohio, 1973.
(6) Principal programs used in this study were: LP-73 data reduction program, T. Ottersen, University of Hawaii, 1973; Full-matrix Least-squares, P. K. Gantzel, R. A. Sparks, and K. N. Trueblood, UCLALS4, American Crystallographic Association Program Library (old) No. 317 (modified); Fourier, C. R. Hubbard, C. O. Quicksall, and R. A. Jacobson, Ames Laboratory Fast Fourier, Iowa State University, 1971, modified; C. K. Johnson, ORTEP, Report ORNL-3794, Oak Ridge National Laboratory, Oak Ridge, Tenn., 1965.
(7) K. Seff, *Acc. Chem. Res.*, **9**, 121 (1976).
(8) I. E. Maxwell and A. Baks, *Adv. Chem. Ser.*, **No. 121**, 87 (1973).
(9) Loewenstein, W., *Am. Mineral.*, **39**, 92 (1954).

Roger L. Firor, Karl Seff*
Chemistry Department, University of Hawaii
Honolulu, Hawaii 96822

Received April 8, 1976

Resonance Raman Spectroscopy with Unsymmetrically Isotopic Ligands. Differentiation of Possible Structures of Hemerythrin Complexes

Sir:

Resonance Raman spectroscopy has been used successfully to probe chromophoric functional centers in several metalloproteins. With the nonheme oxygen-carrier hemerythrin, the vibrational frequencies revealed by resonance Raman lead to an assignment of a peroxide-type, O_2^{2-}, electronic state for the bound dioxygen.[1,2] It also has been apparent to us that unsymmetrically labeled isotopic ligands (e.g., $^{16}O^{18}O$, and $^{15}N^{14}N^{14}N^-$) might be employed to discriminate among alternative geometric arrangements of ligands at the functional site.

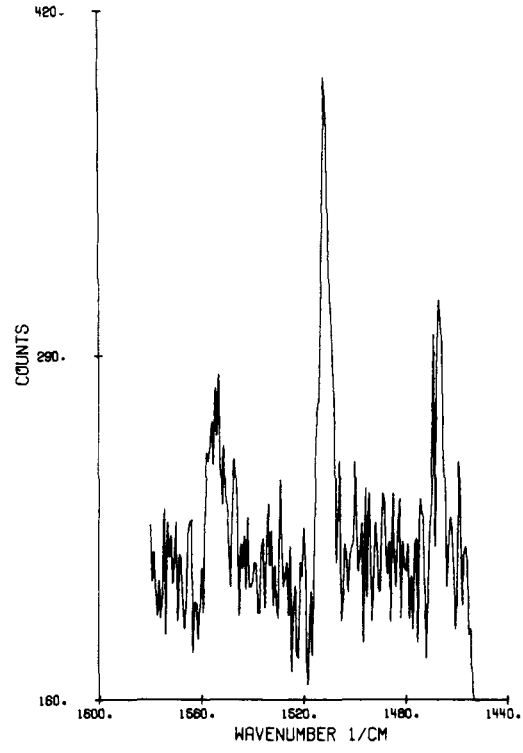

Figure 1. Raman spectrum in the ν_{O-O} region of 58 atom % ^{18}O oxygen gas. Spectrum obtained through a sealed glass ampoule with 90° scattering geometry: laser excitation, 514.5 nm, 150 mW; 3 cm^{-1} spectral slit.

With dioxygen as ligand, the following structural representations have been suggested:[3-8]

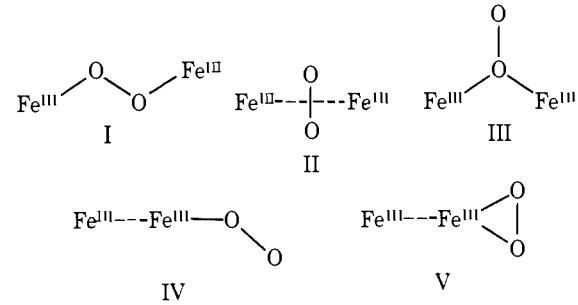

With $^{16}O^{18}O$, single symmetric O–O and Fe–O stretching frequencies, ν_{OO} and ν_{Fe-O}, respectively, would be expected for structures I, II, and V, whereas ν_{OO} and ν_{Fe-O} should each be doublets if dioxygen is bound as shown in III or IV because of the two possible modes of attachment of the unsymmetrical ligand. In view of the difficulty in obtaining a sample of pure $^{16}O^{18}O$, the experiments were performed with a mixture of the isotopic species $^{16}O_2$, $^{16}O^{18}O$, and $^{18}O_2$ (58 atom % ^{18}O from Miles Laboratories). A Raman spectrum of the gaseous dioxygen sample (Figure 1) reveals relative peak heights and relative peak areas of 1:2.6:1.4 each, for the O–O stretch of $^{16}O_2$, $^{16}O^{18}O$, and $^{18}O_2$, respectively. The ν_{O-O} region of the resonance Raman spectrum of oxyhemerythrin prepared with this isotopic mixture of dioxygen gas should resemble Figure 1 if structure I, II, or V is a correct representation. Instead we see in the resonance Raman spectrum of oxyhemerythrin (4 mM in 0.1 M Tris-cacodylate, pH 8) prepared with this same dioxygen sample (Figure 2) three bands in the O_2 stretching region with relative areas of 1:2.7:1.5 but with the central peak

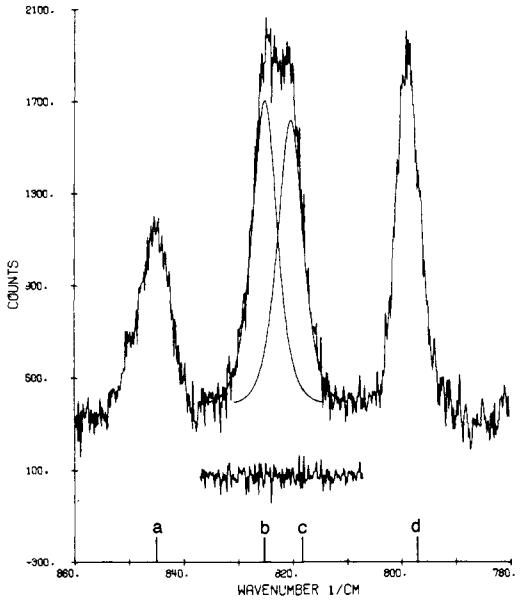

Figure 2. Resonance Raman spectrum in the ν_{O-O} region of oxyhemerythrin prepared with 58 atom % ^{18}O gas: laser excitation, 514.5 nm, 250 mW; 2 cm^{-1} spectral slit. The smooth curves represent deconvolution of the 822-cm^{-1} feature into two components. The difference between observed and fitted curves is shown below the spectrum near 822 cm^{-1}. The vertical lines a, b, c, and d show the calculated peak positions for models III and IV of Fe-$^{16}O_2$ (845 cm^{-1}), Fe-^{16}O-^{18}O (825 cm^{-1}), Fe-^{18}O-^{16}O (818 cm^{-1}), and Fe-$^{18}O_2$ (797 cm^{-1}), respectively.

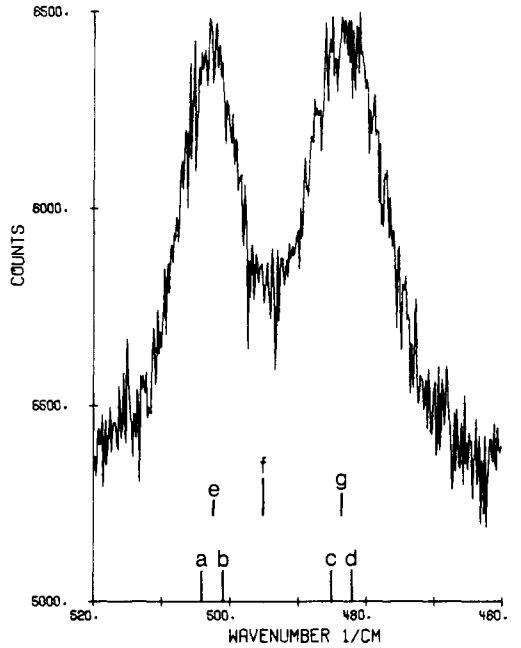

Figure 3. Resonance Raman spectrum in the ν_{Fe-O} region of oxyhemerythrin prepared with 58 atom % ^{18}O gas. Spectral conditions as described in legend to Figure 2. Vertical lines a, b, c, and d show the calculated peak positions for models III and IV of Fe-$^{16}O_2$ (504 cm^{-1}), Fe-^{16}O-^{18}O (501 cm^{-1}), Fe-^{18}O-^{16}O (485 cm^{-1}), and Fe-$^{18}O_2$ (482 cm^{-1}), respectively. Vertical lines e, f, and g show for model V the calculated peak positions and estimated relative intensities of the $^{16}O_2$ (502 cm^{-1}, 1), $^{16}O^{18}O$ (495 cm^{-1}, 2.2), and $^{18}O_2$ (489 cm^{-1}, 1.3) complexes, respectively.

much reduced in height compared to that in Figure 1. Furthermore, the central peak, which represents ν_{O-O} for $^{16}O^{18}O$, is significantly broader (10 cm^{-1} at half height) than the $^{16}O_2$ (7 cm^{-1}) and $^{18}O_2$ (5 cm^{-1}) peaks, and the top is flattened with a slight central depression. These observations indicate that two closely spaced features contribute to the 822-cm^{-1} band. In fact, a good least-squares fit of this band may be achieved by the use of two components of 5.4 cm^{-1} width, at half height,

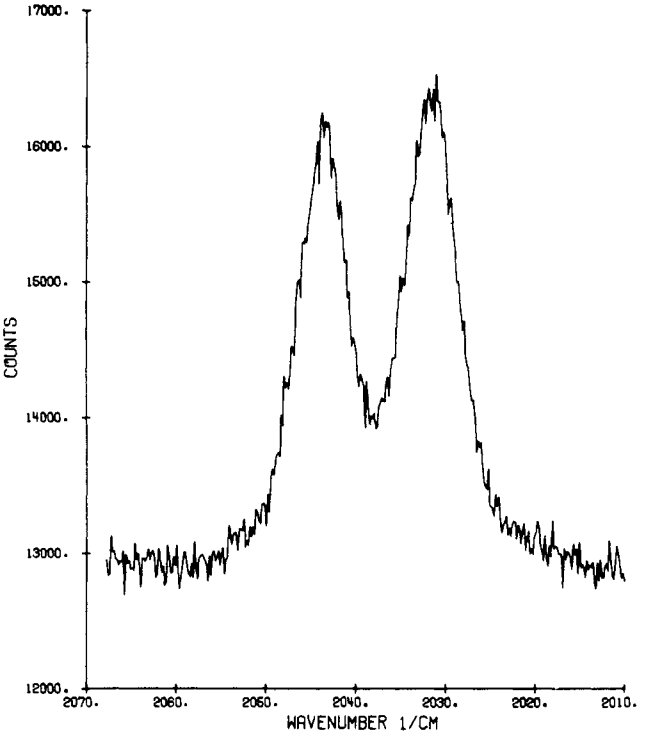

Figure 4. Resonance Raman spectrum in the $\nu_{N\equiv N}$ region of azidomethemerythrin prepared with $K^{15}N^{14}N^{14}N$: laser excitation 488.0 nm, 250 mW; 2 cm^{-1} spectral slit.

separated by 5 cm^{-1} (Figure 2). The occurrence of two closely spaced features in this region is consistent with structures III and IV but not with the others, as depicted, which require only one ν_{OO} for the $^{16}O^{18}O$ protein complex.

Further support for the correctness of structures III and IV is provided by the calculated frequencies for $^{16}O^{18}O$ in various geometries. Values of the simple valence force constants f_{O-O} and f_{Fe-O} were calculated[9] for each of the model structures from data on the $^{16}O_2$ and $^{18}O_2$ protein complexes, and, where it was needed, an Fe-O-O bending force constant was estimated as $0.1f_{Fe-O}$. These force constants were then applied to the calculation of frequencies for the $^{16}O^{18}O$ model structures. As may be seen in Figure 2, the results for models III and IV are in very good agreement with the observed spectrum.

The Fe-O stretching region in the vicinity of 490 cm^{-1} also provides clear evidence for the occurrence of structures such as III and IV. For these two structural models, vibrational analyses demonstrate that the Fe-^{16}O-^{18}O stretch should nearly overlap that of Fe-^{16}O-^{16}O, and a similar near coincidence is calculated for Fe-^{18}O-^{16}O with Fe-^{18}O-^{18}O. The net result is that two composite bands are expected for structures III and IV. By contrast the other structural models require three bands in this region, with the central peak, which is associated with the $^{16}O^{18}O$ species, being the most intense. The calculated and observed peak positions and intensities presented in Figure 3 demonstrate the correctness of structural models III or IV.

A corresponding experiment was performed with another unsymmetrically isotopic ligand, $^{15}N^{14}N^{14}N^-$, in place of $^{16}O^{18}O$. Examination of the resonance Raman spectrum of azidomethemerythrin (9 mM in 0.1 M Tris-cacodylate buffer, pH 7.6) prepared with $K^{15}N^{14}N^{14}N$ (99% isotopic purity from Koch Isotopes Inc.) reveals two clearly resolved peaks[10] in the azide asymmetric stretching $\nu_{N\equiv N}$ region, Figure 4. This spectrum is incompatible with a structure such as VI, but is consistent with either VII or VIII which are analogues of III and IV.

Thus these new spectra indicate that O_2 and N_3^- are bound in analogous geometric dispositions at the functional site of

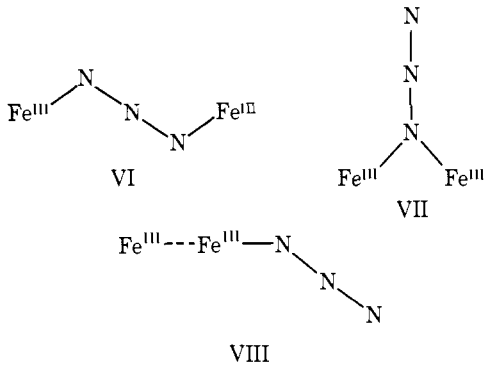

VI VII VIII

hemerythrin, and that the correct structures contain individual O and N atoms in nonequivalent positions.[10-12]

References and Notes

(1) J. B. R. Dunn, D. F. Shriver, and I. M. Klotz, *Proc. Natl. Acad. Sci. U.S.A.*, **70**, 2582 (1973).
(2) J. B. R. Dunn, D. F. Shriver, and I. M. Klotz, *Biochemistry*, **14**, 2689 (1975).
(3) I. M. Klotz and T. A. Klotz, *Science*, **121**, 477 (1955).
(4) S. Keresgtes-Nagy and I. M. Klotz, *Biochemistry*, **4**, 919 (1965).
(5) K. Garbett, D. W. Darnall, I. M. Klotz, and R. J. P. Williams, *Arch. Biochem. Biophys.*, **135**, 419 (1969).
(6) J. W. Dawson, H. B. Gray, H. E. Hoenig, G. R. Rossmann, J. M. Schredder, and R. H. Wang, *Biochemistry*, **11**, 461 (1972).
(7) M. Y. Okamura and I. M. Klotz in "Inorganic Biochemistry" G. L. Eichhorn, Ed., Elsevier, New York, N.Y., 1973, pp 320-343.
(8) J. B. R. Dunn, Ph.D. Dissertation, Northwestern University, 1974.
(9) E. B. Wilson, J. C. Decius, and P. C. Cross, "Molecular Vibrations", McGraw-Hill, New York, N.Y., 1955. For structures I, III, and IV, Fe–O–O angles of 120° were assumed. For all structures, a bond distance of 1.9 Å was assumed for Fe–O and 1.45 Å for O–O.
(10) The observed splittings of ν_{Fe-O} and of $\nu_{N\equiv N}$ are too large to be ascribed to hydrogen bonding to, or protonation of, one of the O atoms in I, II, or V or one of the N atoms in VI. Furthermore we detect no frequency shifts for $\nu_{N\equiv N}$ or ν_{Fe-N} with azidomethemerythrin dissolved in D_2O in place of H_2O.
(11) It is obvious that unsymmetrically-labeled O_2 could also be used to delineate the disposition of oxygen atoms of dioxygen bound by hemocyanin.
(12) This investigation was supported in part by Grant HL-08299 from the National Heart and Lung Institute, U.S. Public Health Service.

Donald M. Kurtz, Jr., Duward F. Shriver, Irving M. Klotz*
Department of Chemistry, Northwestern University
Evanston, Illinois 60201

Received March 22, 1976

High Yield Generation of a Persistent, Saturated Lithium Ketyl in Solution. Characteristic Reactions and Identification by Electron Spin Resonance

Sir:

The classical, still much used method for reducing saturated ketones to alcohols is reduction by means of alkali metals in the presence of proton sources.[1] The mechanism proposed by House for these "dissolving metal reductions" is now generally accepted. In essence, it establishes the sequence, (1) electron transfer to give a ketyl, (2) protonation of the ketyl to give a ketyl radical, and (3) electron transfer to the ketyl radical; dimerizations compete with steps 2 and 3. The ketone dianion intermediates proposed some time ago by Barton[2] are now excluded. In acidic media, the location of the protonation step is to some extent uncertain and, conceivably, important reactions of the ketyls could proceed undetected.

In principle, the lifetime of the ketyls should be longer if the reduction were carried out in nonacidic media. Suitably substituted ketyls should be persistent[3] and it should be possible to show whether further reduction is possible. Study of the chemistry of ketyls in nonacidic media could begin with that of the reactions of persistent ketyls with a variety of reagents.

Apart from the early, promising experiments of Favorski and Nazarov,[4] this approach has been neglected although the formation of ketyls from a number of aliphatic ketones and alkali metal mirrors has since been observed in ESR spectroscopic studies.[5] Later chemical studies of aprotic systems are mainly oriented towards favoring the dimerization of the ketyls.[1]

To bridge the gaps between these sets of data, we have combined ESR and chemical studies of several aprotic systems. Here we wish to report that the reaction between 2,2,6,6-tetramethylcyclohexanone (**1**) and excess lithium in unactivated form in THF at ca. −75° leads to near-quantitative formation of "stable" (−75°) solutions of the corresponding lithium ketyl (**1**·$^-$Li$^+$), but does not proceed further, as indicated by chemical reactions ascribed to **1**·$^-$Li$^+$, and as confirmed by observation of **1**·$^-$Li$^+$ by ESR.

The following considerations determined the choice of the alkali metal, the solvents, and of the ketonic substrate. Suspensions or solutions of lithium metal in donor solvents are the most strongly reducing chemical systems. Moreover, lithium can form strong covalent bonds with carbon; ketone dianion-like species with a covalent C–Li bond should be more stable than true dianions.[1] We use ethers with moderate donor properties such as THF or 1,2-dimethoxyethane (DME) which provide solvation of contact-paired and covalently bound lithium, but leave these C–Li bonds intact; these ethers resist well to abstraction of protons and hydrogen atoms. We find that saturated ketones in THF solution readily react with lithium pieces[6] at ca. −75°. For this first study, we chose a highly hindered ketone in order to slow down bimolecular reactions of derived anions, such as reactions with the medium and dimerization (of the ketyl). In order to exclude the possibility of disproportionation,[7] we used a ketone without hydrogen atoms in the α-positions.

Solutions of **1** (ca. 0.2 M) in THF were stirred at ca. −75° with a large excess (20–50 g-atoms per mole of **1**) of lithium under argon. After stirring for varying periods (10 min to 10 h),[8] the remaining lithium was removed, and the cold (−75°) solutions were quenched with deuterium oxide.[9] Workup with water and distillation of the hydrolysates furnished mixtures of **1** and of the corresponding α-deuterated alcohol **2**-*1*-*d* (Scheme I) in 88–92% combined yield.[10] The molar ratio of **1**:**2** in the hydrolysates had an essentially constant value of unity (0.97–1.10) for contact times (THF solution at −75°/lithium) of 1 h and up to 10 h. The aqueous phases of these hydrolysates contained 1.05–1.10 mol of lithium hydroxide per mole of **1** added initially. After contact times of $< \sim 1$ h the hydrolysates contained **1** and **2** in ratios >1. The deuterium content of the **2**-*1*-*d* in the hydrolysates did not depend on the contact time and was 0.88–0.93 D atom per molecule.[11]

The presence of ketone **1**, alcohol **2**, and lithium hydroxide in equimolar amounts in the hydrolysates defines the overall level of reduction of the species in THF solution as that of the lithium ketyl **1**·$^-$Li$^+$. The only sound interpretation is that only this species is present in significant amounts.[12] We conclude that **1**·$^-$Li$^+$ is formed in high yield (the equilibrium **1** ⇌ **1**·$^-$Li$^+$ lies far on the right) and is persistent in solution at −75°. In particular, **1**·$^-$Li$^+$ is not further reduced to any significant extent. Protonation of **1**·$^-$Li$^+$ induces a disproportionation, as predicted by House's mechanism (Scheme I, reaction with deuterium oxide, exchange on workup gives **2**-*1*-*d*).

Reaction of **1** with lithium in THF at −75° for 3 h as before, treatment of the solution with an excess of trimethylsilyl chloride at −75° after removal of the remaining lithium, and stirring for 4 h at −75°, followed by rapid hydrolytic workup and distillation, gave a mixture of **1** and its bis(trimethylsilyl) derivative **3** (Scheme II), in a ~1.2:1 molar ratio, and in addition a little of the trimethylsilyl ether **4**, in ~75% combined yield.